Determining Transmission Characteristics from Shot Noise-Driven Electroluminescence in Single-Molecule Junctions

Angela L. Paoletta[†] and Latha Venkataraman[*,†,‡]

[†]Department of Chemistry, Columbia University, New York 10027, United States
[‡]Department of Applied Physics and Applied Mathematics, Columbia University, New York 10027, United States

*Email: lv2117@columbia.edu

Abstract:

Biased metal-molecule-metal junctions emit light through electroluminescence, a phenomenon at the intersection of molecular electronics and nanoplasmonics. This can occur when the junction plasmon mode is excited by inelastic electron current fluctuations. Here, we simultaneously measure the conductance and electroluminescence intensity from single-molecule junctions with time resolution in a solution environment at room temperature. We use current versus bias data to determine the molecular junction transport parameters, then relate these to the expected current shot noise. We find that the electroluminescence signal accurately matches the theoretical prediction of shot noise-driven emission in a large fraction of the molecular junctions studied. This introduces a novel experimental method for qualitatively estimating finite-frequency shot noise in single-molecule junctions at ambient conditions. We further demonstrate that electroluminescence can be used to obtain the level alignment of the frontier orbital dominating transport in the molecular junction.

Keywords: electroluminescence; shot noise; plasmonics, localized surface plasmon resonance; single-molecule junctions; scanning tunneling microscope

Although noise in measured electronic signals often decreases measurement sensitivity, shot noise provides a critical source of information about conducting devices.[1,2] Shot noise results from the discrete quantization of charge in tunneling current. Measuring this fundamental property provides insight into a device's transmissio conductance measurements alone.[3-8] However, due to the high frequencies of charge fluctuations, measuring shot noise typically requires fast measurement systems and/or cryogenic temperatures[2,3,9,10], although there are a few exceptions.[4,11] In this work, we present an alternative approach, with all experiments done at room temperature and data acquisition rates no faster than 100 kHz. Our experiment design is advantageous because it is easily incorporated into ambient scanning probe setups and enables shot noise measurements without the need for electronic equipment that measures noise typically at high frequencies. Additionally, our shot noise measurements are made in single metal-molecule-metal junctions at room temperature and in solution, opening up the possibility to carry out similar measurements using more complex molecules. We also measure shot noise at optical frequencies, rather than the lower frequencies typically measured in electrical detection.

Here, we present bias-dependent simultaneous transport and electroluminescence studies using molecules that bind to Au electrodes through direct donor-acceptor bonds. As shown in the scheme in Figure 1a, we apply an electrical bias across the junction to drive current through the frontier molecular orbital (in this case the lowest unoccupied molecular orbital or LUMO). Shot noise, fluctuations in the tunneling current, leads to a coupled oscillation of an electron cloud within an electric field, which can excite a localized surface plasmon resonance (LSPR) inherent to this nanostructure. Relaxation of the LSPR results in photon emission, which is referred to as electroluminescence due to the electric excitation source.[12,13] We observe that both tunneling

current and electroluminescence are maximized close to resonant transport. We then show for over 200 junctions that electroluminescence measurements can be used to determine shot noise at optical frequencies and furthermore predict the position of the dominant transport orbital of the molecular junction from the light emission data rather than from current data, as is typically done.

The primary molecule we study is 4,4'-bipyridine (BPY), shown in Figure 1a. This is an extremely well-characterized[14-17] molecule in metal-molecule-metal junctions and many of its properties have already been explored, including transmission characteristics[15,16] and hot-electron conductance enhancement.[18] Importantly, its transmission is well described by a single-level model,[16] which simplifies our transmission and shot noise calculations as discussed later. We measure conductance and electroluminescence simultaneously using a custom scanning tunneling microscope break junction (STM-BJ) technique.[14,19] Light emission intensity is measured by a silicon photomultiplier (SiPM, Excelitas) and reported as a time-resolved photovoltage signal acquired at 40-100 KHz.[20,21] Figure 1b shows a schematic of this experimental setup. For this measurement, we start by pulling the electrodes apart at a low bias after having formed an Au point contact with a conductance greater than 5 G_0. We then hold the electrodes apart as the bipyridine molecule bridges the gap and we increase the bias from 0 to 2.5 V over a 25 ms period (Figure 1c). Photovoltage is a measure of light emission intensity. One millivolt of photovoltage corresponds to approximately 0.004 nW of optical power or $2*10^7$ photons per second. The collected photovoltage signal is a measure of total intensity over the full range of photon energies for which the detector is sensitive (400 to 1300 nm). We can optionally insert a bandpass filter into the beam path to measure emission over a narrow frequency range.

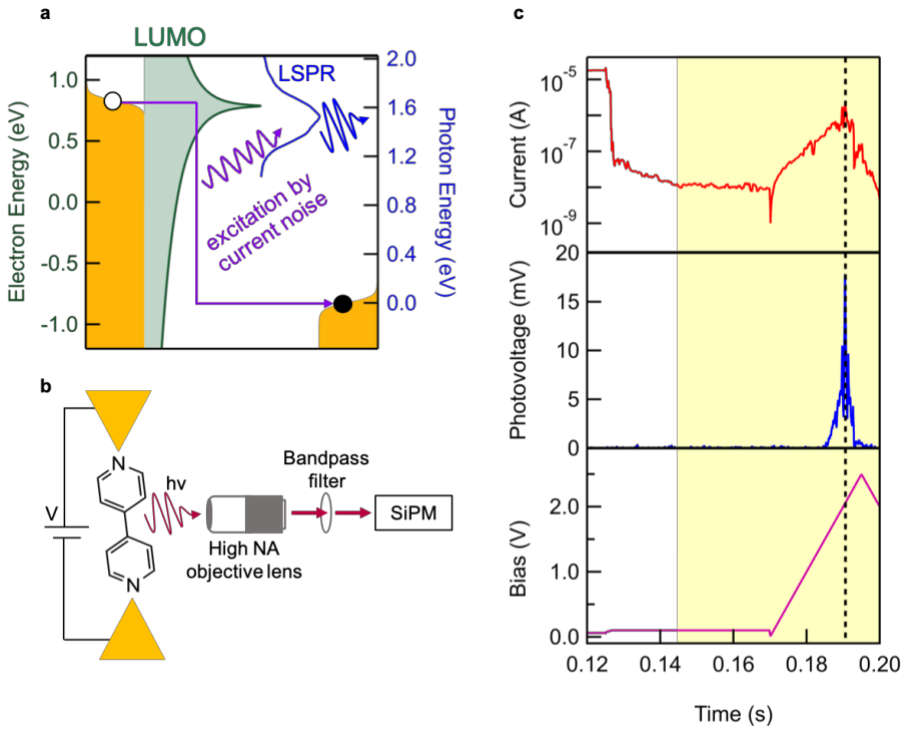

Figure 1. (a) An electron tunnels through the LUMO from substrate to tip, exciting the LSPR through interaction between current fluctuations and the plasmon field. Relaxation of the plasmon emits a photon. (b) 4,4'-bipyridine bridges the gap between Au electrodes. Light emission is collected by a high numerical aperture (NA) objective lens, then directed onto a silicon photomultipler (SiPM). Optionally, a bandpass filter is inserted into the beam path to analyze a select emission frequency. (c) Measured current, photovoltage, and bias for a single trace in which a molecular junction is held while the bias is ramped from 0 to 2.5 V. The electrodes are pulled apart in the white region and held fixed in the yellow region.

In the experiments presented here, the finite-frequency shot noise, function of the photon energy hν, interacts w function given by D(hν). The rough probability der processes can be expressed as:[20-23]

$$_1(\ ) = (\ )(\ ) \qquad (1)$$

$_1(h\nu)$ in Equation 1 is proportional to the photovoltage that we measure, but we expect the magnitude to be different because we only collect some fraction of the total light emitted from the junction. Following the work of Schneider et al.[12] and Lu et al.,[5] $S(h\nu)$, the current spectral density is:

$$(\quad) = \int_{-\frac{|\quad|}{2}}^{\frac{|\quad|}{2}+|\quad|} \quad (\quad)[1 - \quad (\quad - \quad)] \qquad (2)$$

where eV is the energy supplied by the bias, V, and $T(E)$ is the energy-dependent transmission function. We omit the summation over n transport channels as a single-level model has been shown to accurately represent transmission in BP junctions.[16,17] We note that considering the range of biases we use, the transmission function within the expression for shot noise cannot be assumed to be energy-independent as we[20,21] and others[24-26] have done before. We also note that shot noise is maximized at a transmission of 0.5, as has been proven experimentally by Schneider and coworkers.[27] Our molecular junctions operate in low conductance regime (< 0.2 G_0), therefore we expect that shot noise is maximized where transmission or current is maximized.

For each molecular junction, we collect a current versus bias trace and a photovoltage versus bias trace. All traces that sustain a molecular junction during the bias ramp are compiled into the two-dimensional histograms shown in Figure 2. We see that the current increases until 1.8-2.0 V, then decreases thereafter (Figure 2a). This phenomenon, referred to as negative differential resistance (NDR), has been studied before[28-33] and likely indicates that the transmission characteristics of the junction change once the molecular resonance is in the bias window.[30] Figure 2b shows the two-dimensional overlay of measured photovoltage versus bias traces. We also show an overlay of the photoefficiency (light emission per unit of current) versus voltage (Figure 2c), which accounts for the increase in photon emission that comes simply from increasing the number of tunneling electrons, as discussed in our previous work.[21] Photoefficiency typically peaks at or just after the bias at which current is maximized, then decrease thereafter. From analyzing these average histograms of over 1500 junctions, we see that current shot noise can explain a significant portion of the emission. Higher transmission leads to higher current and thus more shot noise and

greater emission intensity. Shot noise is highest where transmission is maximized (but less than 0.5) for the conductance range examined here, so we see that both current and emission are maximized at similar biases. At this bias, we can infer the LUMO is aligned to the edge of the bias window. As a control, we present these histograms for a molecule that does not display strong NDR in the Supporting Information, Figure S4. These junctions do not display a decrease in photoefficiency after a certain bias as there is no strong decrease in current and shot noise.

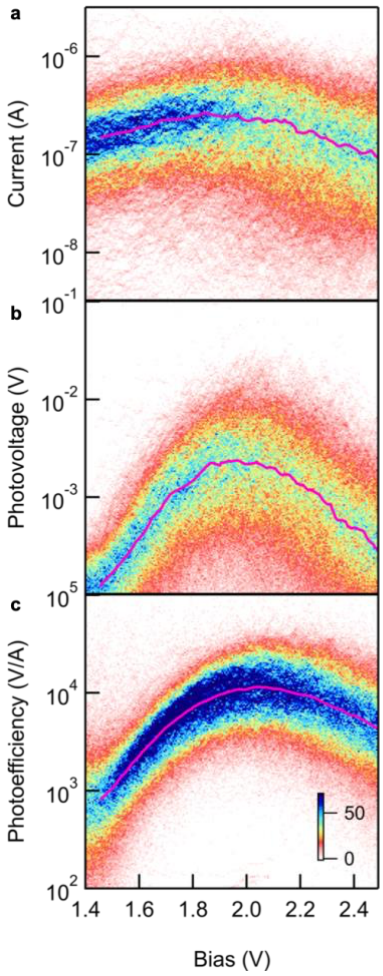

Figure 2. Two-dimensional histograms for over 1500 BP junctions of (a) current versus bias voltage (b) photovoltage versus bias and (c) photoefficiency versus bias. The pink traces show the maximum at each bias. All three panels have the same color range.

Next, we fit individual junction current-voltage data at biases below NDR to a single-level transmission model including thermally-broadened Fermi distributions to determine (the

coupling of the molecule to the leads) and (the energetic position of the molecular orbital relative to the junction Fermi energy) using equations given in Supporting Information Section S4.[34,35] We analyze over 200 junctions and obtain an average of 1.15 eV and average of 0.051 eV. Experimental current versus bias for a single junction is shown in Figure 3a, along with the fit to these data. The transmission function based on the and that best fit the data can be used to calculate the theoretical shot noise-driven light emission using Equation 1 and Equation 2. We can obtain the predicted emission intensi energies for which the SiPM is sensitive (approximately 1 to 3 eV). This is corrected for the energy-dependent sensitivity of the SiPM, as determined by the work of Martinenghi et al.[36] We note that this model only considers single-electron processes and underbias emission. Figure 3b shows the experimental photovoltage versus bias and the calculated emission versus bias using this model and Figure 3c shows the corresponding experimental and calculated photoefficiency versus bias. Clearly, the experimental emission closely follows the calculated shot noise-driven emission for this junction. Figures showing this data with a narrower range of biases are available in the Supporting Information, Figure S2.

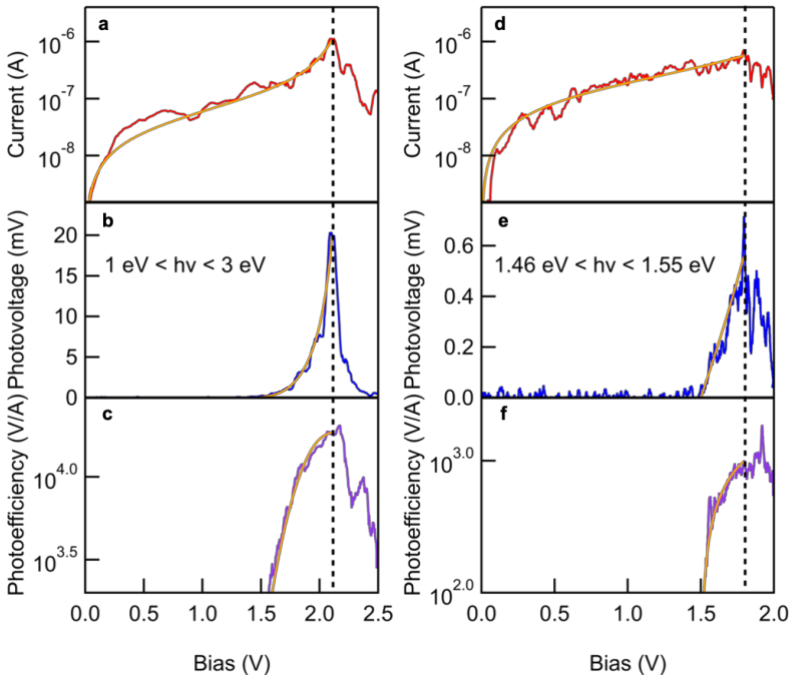

Figure 3. (a) Current versus bias for a single trace. Dashed line indicates the location of NDR. Yellow line is a fit to the data with a single-level model that has = 1.130 eV and = 0.028 eV. (b) Photovoltage versus bias for the trace in (a) along with a fit to the data. (c) Photoefficiency versus bias for the trace in (a) along with a fit to the data. (d) Current versus bias for another trace. Dashed line indicates the location of NDR. Yellow line is a fit to the data with a single-level model that has = 1.165 eV and = 0.051 eV. (e) Photovoltage versus bias measured using a bandpass filter for the trace in (d) along with a fit to the data. (f) Photoefficiency versus bias for the trace in (d) along with a fit to the data.

In Figure 3d-f, we show the same experimental and calculated data as in Figure 3a-c, but now using a bandpass filter to limit our electroluminescence measurement to a narrow energy range of 800 to 850 nm (or 1.46 to 1.55 eV). Knowing the photon energy is critical to our calculations of shot noise from photovoltage, as we will discuss below. But first, we will show that the same initial calculations based on current versus bias data can be done on this set of data using a filter. As in Figure 3a-c, we obtain and by fitting the current versus bias trace, then calculate emission from the shot noise following Equation 1 and Equation 2. For the data in Figure 3e, the calculated emission intensity is for photons of energy 1.5 eV and consequently there is no correction for the energy-dependent sensitivity of the SiPM. Although the exact magnitude of the

photovoltage is not meaningful, scaling the calculated photovoltage by a factor of 0.2 to account for the fact that we don't collect all the li

Given that Equations 1 and 2 fit to our experimental results, we can take this one step further and use the electroluminescence at a particular frequency to obtain a measurement of shot noise in the junction. As we alluded to in the previous paragraph, in doing this calculation it now becomes necessary to use a bandpass filter so that we only measure electroluminescence at a select frequency. We have chosen 1.5 eV because photons with an energy of ~ 1.5 eV are considered underbias for biases greater than 1.5 V. This eliminates the need to consider overbias emission, simplifying our calculations. Without this filter, we cannot equate electroluminescence to shot noise because we would not be able to obtain shot noise as a function of bias.

We thus use the data which allows photovoltage signal only between 800 and 850 nm, which sets $h\nu$ in Equations 1 and 2 $S(h\nu)$ 1.5 eV. Now we have reduced value at each bias rather than a function and we can fit the photovoltage versus bias data to determine of the junction using the following equation:

$$(\quad ,) = \quad ^2 \left[\frac{| \quad | -}{(\varepsilon \quad - \frac{| \quad |}{2})(\varepsilon \quad + \frac{| \quad |}{2} - \quad)} \right] \qquad (3)$$

Figure 4a-d shows two example traces in which the photovoltage versus bias is used to obtain . (Figures with a narrower range of biases are presented in the Supporting Information, Figure S3.) We compare this to as determined from current versus bias. We do this analysis for over 200 junctions and find that matches closely for the majority of traces, with 54% of traces having a difference between of 0.1 eV or less and 82% of traces having a difference of 0.2 eV or less. Figure 4e shows a histogram of these differences. It is clear that the position of the

frontier resonance can be determined from photovoltage in these traces, although our data indicates that electroluminescence in all junctions is not entirely due to shot noise.

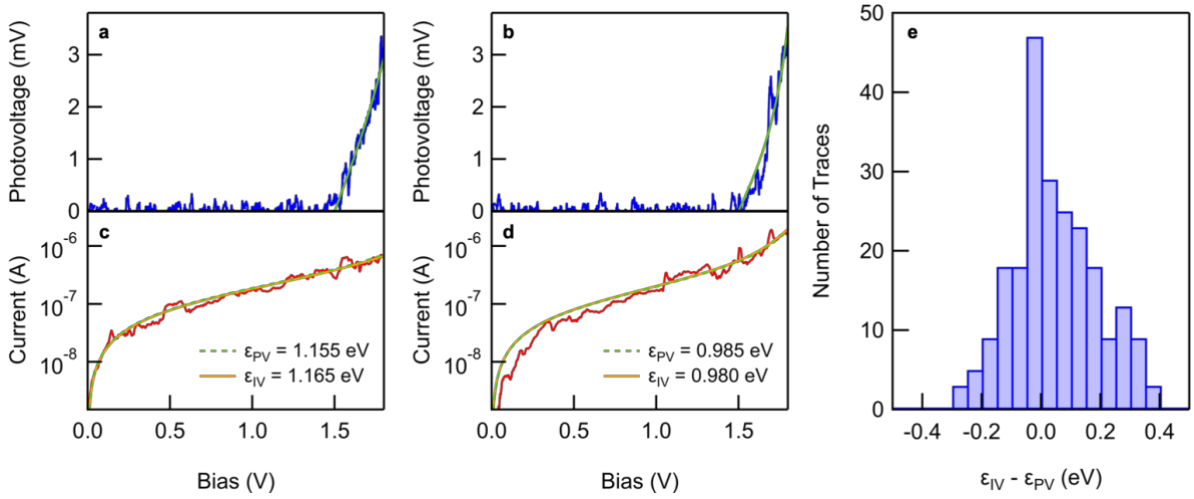

Figure 4. (a, b) Example photovoltage versus bias traces along with fits to the data assuming all light is shot-noise driven emission. (c) Current versus bias corresponding to (a) along with calculated current using = 0.051 eV and determined from fitting the current (orange) or determined from shot-noise (green). (d) Current versus bias corresponding to (b) along with calculated current using = 0.043 eV and determined from fitting the current (orange) and determined from shot-noise (green). (e) Histogram of the difference between and for over 200 traces.

In conclusion, we have measured light emission from BP molecular junctions at room temperature, in ambient conditions and in solution. Our results show that light emission from most junctions matches the theoretically-predicted shot noise-driven electroluminescence, indicating that shot noise-driven plasmonic emission comprises a large portion of the photons emitted from these junctions. We took this finding further by measuring electroluminescence at a particular photon energy, using that data to predict the bias-dependent finite-frequency shot noise of the junction, and determining the energy of the molecular orbital that dominates transmission based on electroluminescence data. We find that for the majority junctions, closely matches , meaning that the position of the molecular orbital dominating transport can be accurately predicted by the junction electroluminescence. This provides a new way of determining

transport parameters in single-molecule junction studies using light emission data rather than current data. Furthermore, this work introduces a new method for estimating shot noise experimentally, using electroluminescence. The work presented here offers a qualitative estimate, but this could be built upon in systems where all light can be collected in order to measure shot noise quantitively without the use of high frequency measurements or cryogenic temperatures.

Supporting Information

STM-BJ technique, electroluminescence setup, additional methods, analysis and data.

Acknowledgements

A.L.P is supported by the National Defense Science and Engineering Graduate Fellowship. This research was supported in part by the National Science Foundation under grant CHE-2023568.

References

1 Mu, A., Shein-Lumbroso, O., Tal, O. & Segal, D. Origin of the Anomalous Electronic Shot Noise in Atomic-Scale Junctions. *J. Phys. Chem. C* **123**, 23853-23862 (2019). https://doi.org/10.1021/acs.jpcc.9b06766

2 Kim, Y. & Song, H. Noise spectroscopy of molecular electronic junctions. *Appl. Phys. Rev.* **8**, 011303 (2021). https://doi.org/10.1063/5.0027602

3 Djukic, D. & Ruitenbeek, J. M. v. Shot Noise Measurements on a Single Molecule. *Nano Lett.* **6**, 789-793 (2006).

4 Wheeler, P. J., Russom, J. N., Evans, K., King, N. S. & Natelson, D. Shot noise suppression at room temperature in atomic-scale Au junctions. *Nano Lett.* **10**, 1287-1292 (2010). https://doi.org/10.1021/nl904052r

5 Lü, J.-T., Christensen, R. B. & Brandbyge, M. Light emission and finite-frequency shot noise in molecular junctions: From tunneling to contact. *Phys. Rev. B* **88**, 045413 (2013). https://doi.org/10.1103/PhysRevB.88.045413

6 Kumar, M. *et al.* Shot noise and magnetism of Pt atomic chains: Accumulation of points at the boundary. *Phys. Rev. B* **88**, 245431 (2013). https://doi.org/10.1103/PhysRevB.88.245431

7 Lumbroso, O. S., Simine, L., Nitzan, A., Segal, D. & Tal, O. Electronic noise due to temperature differences in atomic-scale junctions. *Nature* **562**, 240-244 (2018). https://doi.org/10.1038/s41586-018-0592-2

8 Vardimon, R., Klionsky, M. & Tal, O. Experimental determination of conduction channels in atomic-scale conductors based on shot noise measurements. *Phys. Rev. B* **88**, 161404 (2013). https://doi.org/10.1103/PhysRevB.88.161404

9 Karimi, M. A. *et al.* Shot Noise of 1,4-Benzenedithiol Single-Molecule Junctions. *Nano Lett.* **16**, 1803-1807 (2016). https://doi.org/10.1021/acs.nanolett.5b04848

10 Tewari, S. *et al.* Fast and accurate shot noise measurements on atomic-size junctions in the MHz regime. *Rev. Sci. Instr.* **88**, 093903 (2017). https://doi.org/10.1063/1.5003391

11 Chen, R. *et al.* Shot noise variation within ensembles of gold atomic break junctions at room temperature. *J. Phys. Condens. Matter* **26**, 474204 (2014). https://doi.org/10.1088/0953-8984/26/47/474204

12 Schneider, N. L., Lu, J. T., Brandbyge, M. & Berndt, R. Light emission probing quantum shot noise and charge fluctuations at a biased molecular junction. *Phys. Rev. Lett.* **109**, 186601 (2012). https://doi.org/10.1103/PhysRevLett.109.186601

13 Zhu, W. *et al.* Quantum mechanical effects in plasmonic structures with subnanometre gaps. *Nat. Commun.* **7**, 11495 (2016). https://doi.org/10.1038/ncomms11495

14 Xu, B. & Tao, N. J. Measurement of Single-Molecule Resistance by Repeated Formation of Molecular Junctions. *Science* **301**, 1221-1223 (2003).

15 Quek, S. Y. *et al.* Mechanically controlled binary conductance switching of a single-molecule junction. *Nat. Nano.* **4**, 230-234 (2009). https://doi.org/10.1038/nnano.2009.10

16 Kim, T. *et al.* Determination of energy level alignment and coupling strength in 4,4'-bipyridine single-molecule junctions. *Nano Lett.* **14**, 794-798 (2014). https://doi.org/10.1021/nl404143v

17 Adak, O., Korytar, R., Joe, A. Y., Evers, F. & Venkataraman, L. Impact of Electrode Density of States on Transport through Pyridine-Linked Single Molecule Junctions. *Nano Lett.* **15**, 3716-3722 (2015). https://doi.org/10.1021/acs.nanolett.5b01195

18 Fung, E. D., Adak, O., Lovat, G., Scarabelli, D. & Venkataraman, L. Too Hot for Photon-Assisted Transport: Hot-Electrons Dominate Conductance Enhancement in Illuminated Single-Molecule Junctions. *Nano Lett.* **17**, 1255-1261 (2017). https://doi.org/10.1021/acs.nanolett.6b05091

19 Venkataraman, L., Klare, J. E., Nuckolls, C., Hybertsen, M. S. & Steigerwald, M. L. Dependence of single-molecule junction conductance on molecular conformation. *Nature* **442**, 904-907 (2006). https://doi.org/10.1038/nature05037

20 Fung, E. D. & Venkataraman, L. Too Cool for Blackbody Radiation: Overbias Photon Emission in Ambient STM Due to Multielectron Processes. *Nano Lett.* **20**, 8912-8918 (2020). https://doi.org/10.1021/acs.nanolett.0c03994

21 Paoletta, A. L., Fung, E. D. & Venkataraman, L. Gap Size-Dependent Plasmonic Enhancement in Electroluminescent Tunnel Junctions. *ACS Photonics* **9**, 688-693 (2022). https://doi.org/10.1021/acsphotonics.1c01757

22 Hone, D., Mühlschlegel, B. & Scalapino, D. J. Theory of light emission from small particle tunnel junctions. *Appl. Phys. Lett.* **33**, 203-204 (1978). https://doi.org/10.1063/1.90275

23 Parzefall, M. & Novotny, L. Optical antennas driven by quantum tunneling: a key issues review. *Rep. Prog. Phys.* **82**, 112401 (2019). https://doi.org/10.1088/1361-6633/ab4239

24 Kaasbjerg, K. & Nitzan, A. Theory of light emission from quantum noise in plasmonic contacts: above-threshold emission from higher-order electron-plasmon scattering. *Phys. Rev. Lett.* **114**, 126803 (2015). https://doi.org/10.1103/PhysRevLett.114.126803

25 Tobiska, J., Danon, J., Snyman, I. & Nazarov, Y. V. Quantum tunneling detection of two-photon and two-electron processes. *Phys. Rev. Lett.* **96**, 096801 (2006). https://doi.org/10.1103/PhysRevLett.96.096801

26 Cui, L., Zhu, Y., Nordlander, P., Di Ventra, M. & Natelson, D. Thousand-fold Increase in Plasmonic Light Emission via Combined Electronic and Optical Excitations. *Nano Lett.* **21**, 2658-2665 (2021). https://doi.org/10.1021/acs.nanolett.1c00503

27 Schneider, N. L., Schull, G. & Berndt, R. Optical probe of quantum shot-noise reduction at a single-atom contact. *Phys Rev Lett* **105**, 026601 (2010). https://doi.org/10.1103/PhysRevLett.105.026601

28 Xu, B. & Dubi, Y. Negative differential conductance in molecular junctions: an overview of experiment and theory. *J. Phys. Condens. Matt.* **27**, 263202 (2015). https://doi.org/10.1088/0953-8984/27/26/263202

29 Chen, J., Reed, M. A., Rawlett, A. M. & Tour, J. M. Large On-Off Ratios and Negative Differential Resistance in a Molecular Electronic Device. *Science* **286**, 1550-1552 (1999).

30 Fung, E. D. *et al.* Breaking Down Resonance: Nonlinear Transport and the Breakdown of Coherent Tunneling Models in Single Molecule Junctions. *Nano Lett.* **19**, 2555-2561 (2019). https://doi.org/10.1021/acs.nanolett.9b00316

31 Kuang, G. *et al.* Negative Differential Conductance in Polyporphyrin Oligomers with Nonlinear Backbones. *J. Am. Chem. Soc.* **140**, 570-573 (2018). https://doi.org/10.1021/jacs.7b11016

32 Perrin, M. L. *et al.* Large negative differential conductance in single-molecule break junctions. *Nat. Nano.* **9**, 830-834 (2014). https://doi.org/10.1038/nnano.2014.177

33 Xiao, X., Nagahara, L. A., Rawlett, A. & Tao, N. Electrochemical Gate-Controlled Conductance of Single Oligo(phenylene ethynylene)s. *J. Am. Chem. Soc.* **127**, 5 (2005).

34 Capozzi, B. *et al.* Mapping the Transmission Functions of Single-Molecule Junctions. *Nano Lett.* **16**, 3949-3954 (2016). https://doi.org/10.1021/acs.nanolett.6b01592

35 Datta, S. *Electronic Transport in Mesoscopic Systems*. (Cambridge University Press, 1995).

36 Martinenghi, E. *et al.* Time-resolved single-photon detection module based on silicon photomultiplier: A novel building block for time-correlated measurement systems. *Rev. Sci. Instr.* **87**, 073101 (2016). https://doi.org/10.1063/1.4954968

TOC Graphic